Pergamon

Acta metall. mater. Vol. 42, No. 3, pp. 879–886, 1994

0956-7151/94 $6.00 + 0.00

RELATIONSHIP BETWEEN ROLLING TEXTURES AND SHEAR TEXTURES IN F.C.C. AND B.C.C. METALS

M. HÖLSCHER, D. RAABE and K. LÜCKE

Institut für Metallkunde und Metallphysik, Kopernikusstr. 14, RWTH Aachen, W-52074 Aachen, Germany

(Received 8 February 1993; in revised form 16 July 1993)

Abstract—The rolling and shear textures of aluminium (f.c.c.) and Fe–16% Cr (b.c.c.) have been compared. First a 90° rotation relationship about the transverse direction was found experimentally between the stable orientations of the rolling textures and the shear textures. This was explained with the symmetry of the glide systems and the orientation relationship between both coordinate systems. Second for both kinds of deformation namely rolling and shear a 90° rotation relationship about the transverse direction was also found between the stable b.c.c. and f.c.c. orientations. This was explained with the Taylor theory and the Sachs model making use of the orientation relationship between f.c.c. and b.c.c. glide systems.

Résumé—Les textures de laminage et de cission de l'aluminium et d'un alliage Fe–16% Cr ont été comparées. Premièrement une relation de rotation de la direction transversale a été trouvée expérimentalement entre les orientations stables de laminage et de cission. Celleci est expliquée par la symmétrie des systèms de glissement et la relation du rotation entre les deux "systèmes de coordonées. En plus, pour les deux modes de déformation la même relation de rotation de 90° autour de la direction transversale a été trouvée entre les orientations stables cc et cfc. Cette relation est expliquée à l'aide de la théorie de Taylor et du modèle de Sachs en utilisant la relation d'orientation entre les systèmes de glissement cfc et cc.

Zusammenfassung—Die Walz- und Schertexturen von Aluminium (k.f.z.) und Fe–16% Cr (k.r.z.) wurden vergleichend untersucht. Erstens wurde bei beiden Materialien experimentell eine 90° Rotationsbeziehung um die Querrichtung zwischen den stabilen Orientierungen der Walz- und der Schertexturen gefunden. Diese wird über die Symmetrie der Gleitsysteme und die Rotationsbeziehung der entsprechenden Koordinatensysteme erklärt. Zweitens wurde sowohl beim Walzen, als auch bei den Scherverformungen eine 90° Rotation um die Querrichtung zwischen den stabilen k.r.z. und k.f.z. Endorientierungen gefunden. Diese Orientierungsbeziehung wird theoretisch mittels der Taylortheorie und des Sachsmodels auf der Basis der Orientierungsbeziehung der k.f.z.- und der k.r.z. Gleitsysteme erklärt.

1. INTRODUCTION

The texture development during rolling and shear deformation of f.c.c. and b.c.c. metals has been thoroughly investigated in the last 30 years (e.g. [1, 2]). Whereas its evolution is well understood in terms of the Sachs- [3], Taylor- [4] and "Relaxed Constraints" Taylor models [5], only a few remarks attribute to the relations between f.c.c. and b.c.c. textures on the one hand [6, 7] and shear and rolling textures on the other hand.

Since mostly the pole figures with the highest intensities are presented ({111} for f.c.c. and {110} for b.c.c.) the comparison of these textures is complicated and similarities do hardly become obvious. The introduction of the orientation distribution function (ODF) [8] was assumed to overcome this shortcoming since here the orientation densities instead of the pole densities are presented. But in order to display the most interesting features of the textures the sections through the Euler angle space (φ_1,Φ,φ_2) were often chosen differently for f.c.c. (φ_2-sections) and b.c.c. (φ_1-sections) so that no direct comparison of the textures was possible.

The aim of the present work is first to demonstrate experimentally that there is a strong equivalence between the four types of textures namely rolling and shear textures on the one hand and between f.c.c. and b.c.c. materials on the other hand, and second to give a theoretical explanation for the observed correspondence.

2. MATERIALS AND METHODS

As example for f.c.c. aluminium (99.9%) and for b.c.c. a ferritic steel with 16% chromium (FeCr) were chosen. Aluminium (Al) possesses a high stacking fault energy and will therefore mainly deform by {111}⟨110⟩ slip and not by twinning. Since alloy elements favour slip on {110} planes in iron [9], {011}⟨111⟩ systems are supposed to be dominantly active in FeCr. Both materials were cold rolled homogeneously to 75% reduction, i.e. for every pass (reduction Δd, roll diameter r) the ratio between the

contact length of the strip with the roll l_d and the thickness d_0 obeyed

$$1.5 \leqslant \frac{l_d}{d_0} < 3, \quad \frac{l_d}{d_0} \approx \frac{\sqrt{(r \cdot \Delta d)}}{d_0} \tag{1}$$

The shear textures were produced by inhomogeneous rolling deformation with very high reductions per pass. Applying this procedure yields a pronounced shear texture at the sub-surface layer of the sheets. For Al this was achieved by rolling at room temperature on a laboratory rolling mill, whereas for FeCr a commercial hot band could be used, since during the last hot rolling steps no phase transformation and thus no change of the deformation texture occurs.

The textures were determined by measuring incomplete X-ray pole figures in the back reflection mode [10]. From a set of four pole figures ({111}, {200}, {220}, {311} for Al and {110}, {200}, {112}, {103} for FeCr) the ODF was calculated using the series expansion method ($l_{max} = 22$) [8]. The here presented, symmetric pole figures are recalculated from the ODF. Since the stress state at the surface is rotated 45° about the transverse direction when compared to the stress state in the center the surface textures are also symmetrical so that the recalculated pole figures can be considered.

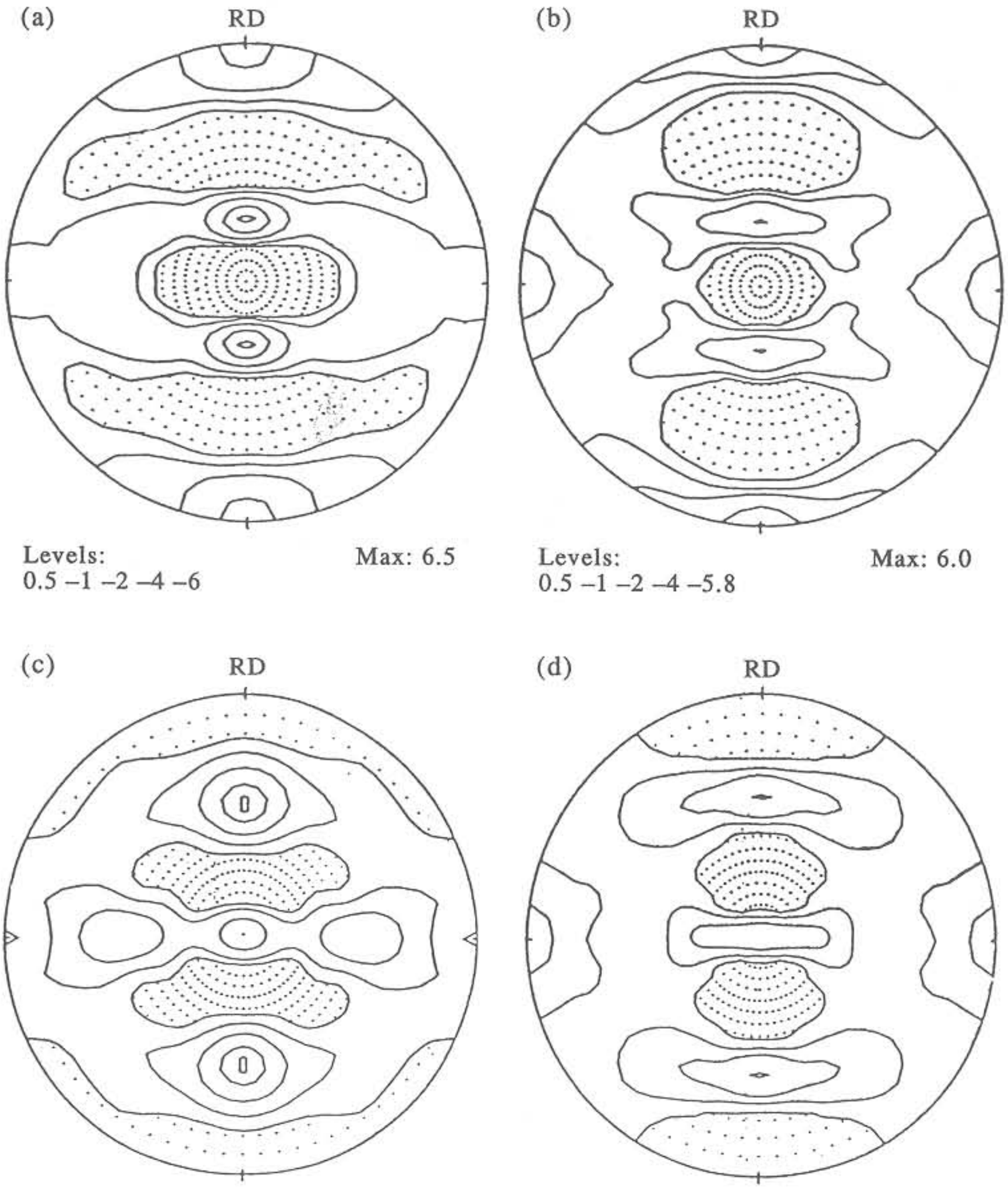

Fig. 1. Recalculated pole figures of aluminium and Fe–16% Cr. RD = rolling direction. (a) Aluminium, 75% homogeneously cold rolled, {111} pole figure. (b) Fe–16% Cr, 75% homogeneously cold rolled, {110} pole figure. (c) Aluminium, 75% inhomogeneously cold rolled, i.e. sheared, {111} pole figure. (d) Fe–16% Cr, 75% inhomogeneously hot rolled, i.e. sheared, {110} pole figure.

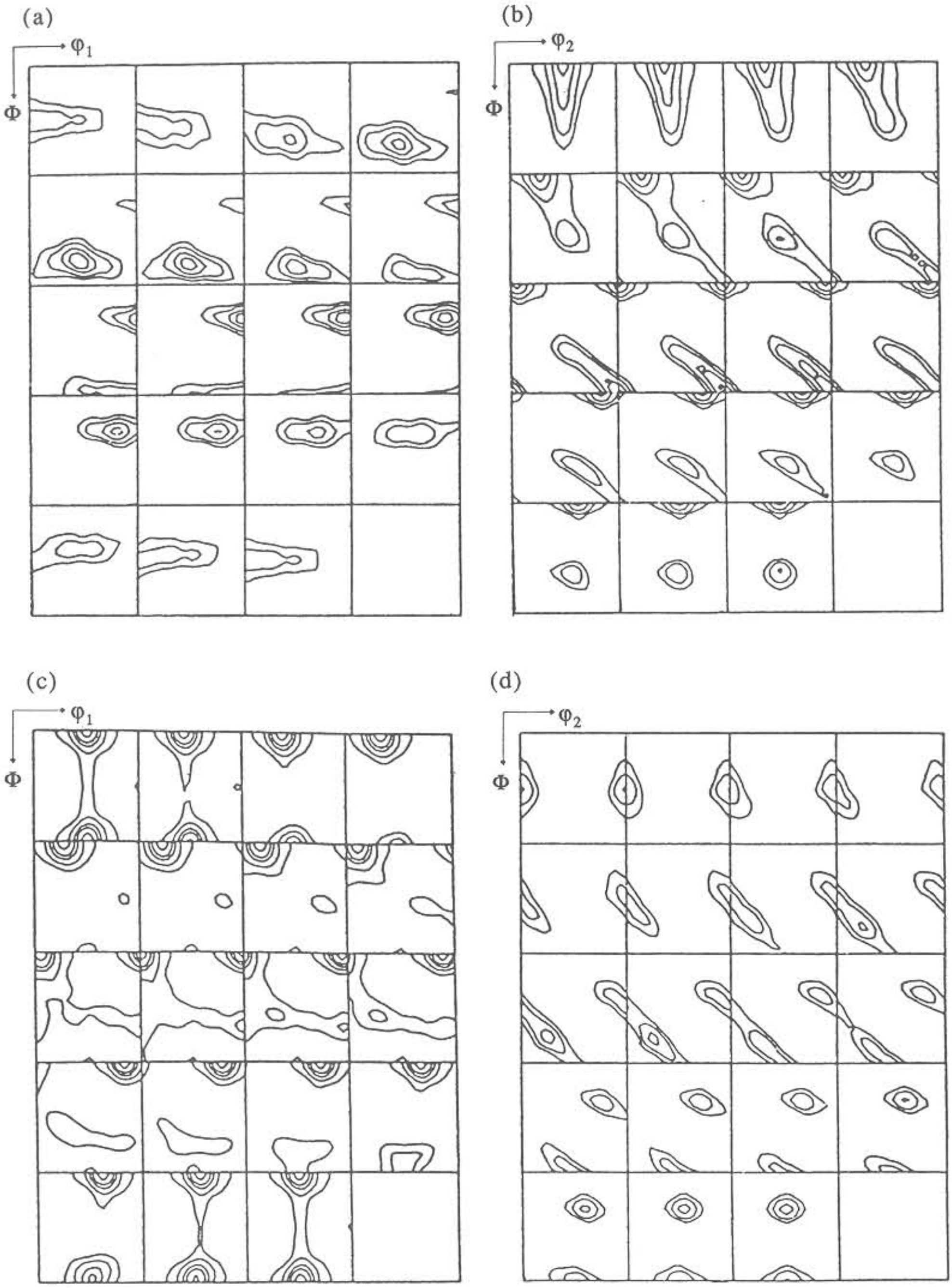

Fig. 2. Orientation distribution functions (ODFs) of aluminium and Fe–16% Cr. (a) Aluminium, 75% homogeneously cold rolled, φ_2-sections. (b) Fe–16% Cr, 75% homogeneously cold rolled, φ_1-sections. (c) Aluminium, 75% inhomogeneously cold rolled, i.e. sheared, φ_2-sections. (d) Fe–16% Cr, 75% inhomogeneously hot rolled, i.e. sheared, φ_1-sections.

3. EXPERIMENTAL RESULTS AND EVALUATION

In Fig. 1(a,b) the {111} pole figure for Al and the {110} pole figure for FeCr are depicted for the homogeneously rolled samples, whereas Fig. 1(c,d) expose the pole figures obtained from the surface layers of the inhomogeneously rolled Al and FeCr. In Fig. 2(a–d) the corresponding ODFs are shown in φ_1-sections for b.c.c. and in φ_2-sections for f.c.c.

Regarding the pole figures and ODFs of Figs 1 and 2, one realizes that all four textures look completely different. If however the important components are described by Miller indices (Table 1), one can observe two features. First the rolling components of f.c.c. and b.c.c. are nearly identical, if the Miller indices are

simply interchanged from $\{hkl\}\ \langle uvw\rangle$ into $\{uvw\}\ \langle hkl\rangle$ [6, 7]. Second, for both materials again nearly identical components are obtained when the Miller indices between the prominent rolling and shear orientations are exchanged. This means the f.c.c. rolling components coincide with the b.c.c. shear components and vice versa. Such a transformation of indices corresponds to an interchange of R and N and thus describes a rotation of 90° about the transverse direction (T). This means a 90° rotation of stable orientations about T holds for two kinds of transformation. First for rolling or shear components from f.c.c. to b.c.c. and vice versa. Second for both f.c.c. and b.c.c. between rolling and shear orientations.

To study these relationships the {111} pole figures for all four samples [Fig. 1(a–d)] were recalculated from the ODF data. To achieve comparability the b.c.c. rolling texture and the f.c.c. shear texture had to be rotated 90° about T whereas for the b.c.c. shear texture no rotation was necessary (Fig. 3). The ODFs were rotated in the same way and plotted in φ_2-sections (Fig. 4). The pole figures as well as the ODFs are very similar to each other.

4. INTERPRETATION OF THE TEXTURE RELATIONSHIPS

The here demonstrated simple 90° rotation relationships between f.c.c. and b.c.c. deformation textures on the one hand and between rolling and shear textures on the other hand must be caused by principal equivalences during deformation.

4.1. Orientation change by slip

First, the relationship between the f.c.c. and b.c.c. rolling texture development of 90° about T will be examined. The experimentally found orientation changes can be tackled by the Sachs model [3] and by the Taylor "Relaxed Constraints" model [5], which differ in the way how the active slip systems and the amount of slip is determined. All models are able to calculate the resulting antisymmetric part of the displacement gradient tensor, i.e. the orientation change. If it can be shown that the 90° rotation relationship between f.c.c. and b.c.c. is valid for an orientation change by slip on one system it also holds for the linear combination of several glide systems. The shear γ on a slip system with the unit normal vector of the glide plane $n=(n_1,n_2,n_3)$ and the slip vector $b=(b_1,b_2,b_3)$ will change any vector A as follows

$$A' = A + \gamma(A\cdot n)\cdot b \tag{2a}$$

or in case of z activated glide sytems

$$A' = A + \sum_{s=1}^{z} [\gamma^s (A\cdot n^s)\cdot b^s]. \tag{2b}$$

In order to calculate the orientation change during rolling a triple of vectors A_R, A_T, A_N, lying parallel to the orthonormal sample coordinate system (R, T and N) is chosen

$$R=\begin{pmatrix}1\\0\\0\end{pmatrix},\quad T=\begin{pmatrix}0\\1\\0\end{pmatrix},\quad N=\begin{pmatrix}0\\0\\1\end{pmatrix} \tag{3}$$

Executing the shear γ on one slip system the vectors A_R, A_T, and A_N generally change their length and direction into A'_R, A'_T, and A'_N if the crystal coordinate system is fixed. After the deformation the new unit vectors of the sample are thus R', T', and N'. Following the constraints caused by the rolling mill however, R and N have to remain invariant during rolling, so that equation (4) is valid.

$$R'\| A'_R;\quad N'\|(A'_R\times A'_T);\quad T'\|(N'\times R') \tag{4}$$

With the help of equation (2) the orientation change of the sample coordinate system with respect to the crystal system can be calculated. With regard to transparency the orientation change due to mobilization of one glide system is tackled. The calculations remain however linear if more slip systems are active

$$R'\| R + \gamma(R\cdot n)\cdot \mathrm{b} \tag{5a}$$

$$T'\| T + \gamma(T\cdot n)\cdot b \tag{5b}$$

$$b\cdot n = 0 \tag{5c}$$

$$N'\| R'\times T' \tag{6a}$$

$$N'\|[R+\gamma(R\cdot n)\cdot b]\times[T+\gamma(T\cdot n)\cdot b] \tag{6b}$$

$$N'\|(R\times T)+\gamma(T\cdot n)(R\times b)+\gamma(R\cdot n)(b\times T) \tag{6c}$$

$$N'\| N+\gamma[(T\cdot n)(R\times b)+(R\cdot n)(b\times T)] \tag{6d}$$

$$N'\| N+\gamma[-n_2(b\times R)+n_1(b\times T)] \tag{6e}$$

$$N'\| N+\gamma(b\times(n_1 T-n_2 R)] \tag{6f}$$

$$N'\| N+\gamma(-b_3 n) \tag{6g}$$

$$N'\| N-\gamma(N\cdot b)\cdot n. \tag{6h}$$

With equation (6h), the above mentioned interchange of the glide systems between f.c.c. and b.c.c. namely

$$b_{\mathrm{b.c.c.}} = n_{\mathrm{f.c.c.}};\quad n_{\mathrm{b.c.c.}} = -b_{\mathrm{f.c.c.}} \tag{7}$$

Table 1. Main orientations in Fe–16% Cr and aluminium after rolling and shear deformation

Preferred orientations	FeCr Rolling	FeCr Shear	Al Rolling	Al Shear
{001} ⟨110⟩	+	−	−	+
{112} ⟨110⟩	+	−	−	(+)
{111} ⟨110⟩	+	−	−	(+)
{111} ⟨112⟩	+	−	−	+
{11 11 8} ⟨4 4 11⟩	(+)	−	−	+
{011} ⟨100⟩	−	+	+	−
{011} ⟨211⟩	−	+	+	−
{011} ⟨111⟩	−	+	(+)	−
{112} ⟨111⟩	−	+	+	−
{4 4 11} ⟨11 11 8⟩	−	+	+	−

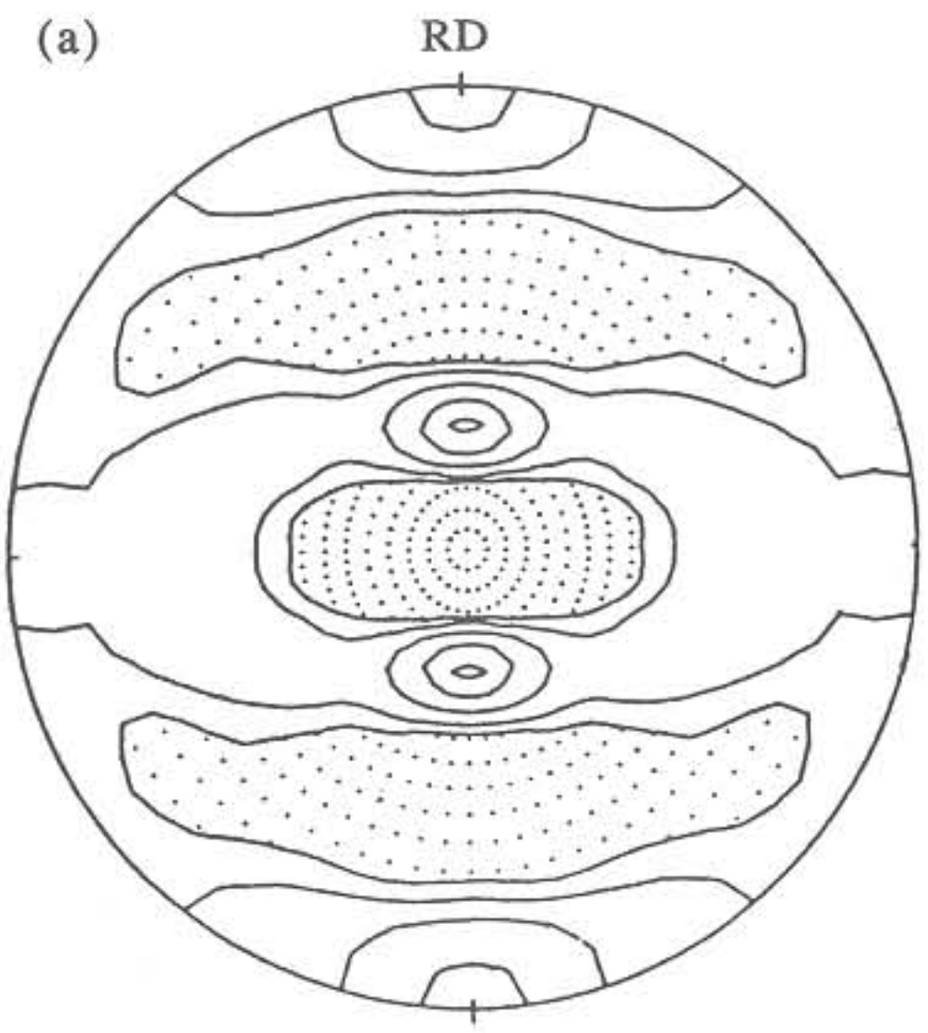

Levels:
0.5 –1 –2 –4 –6

Max: 6.5

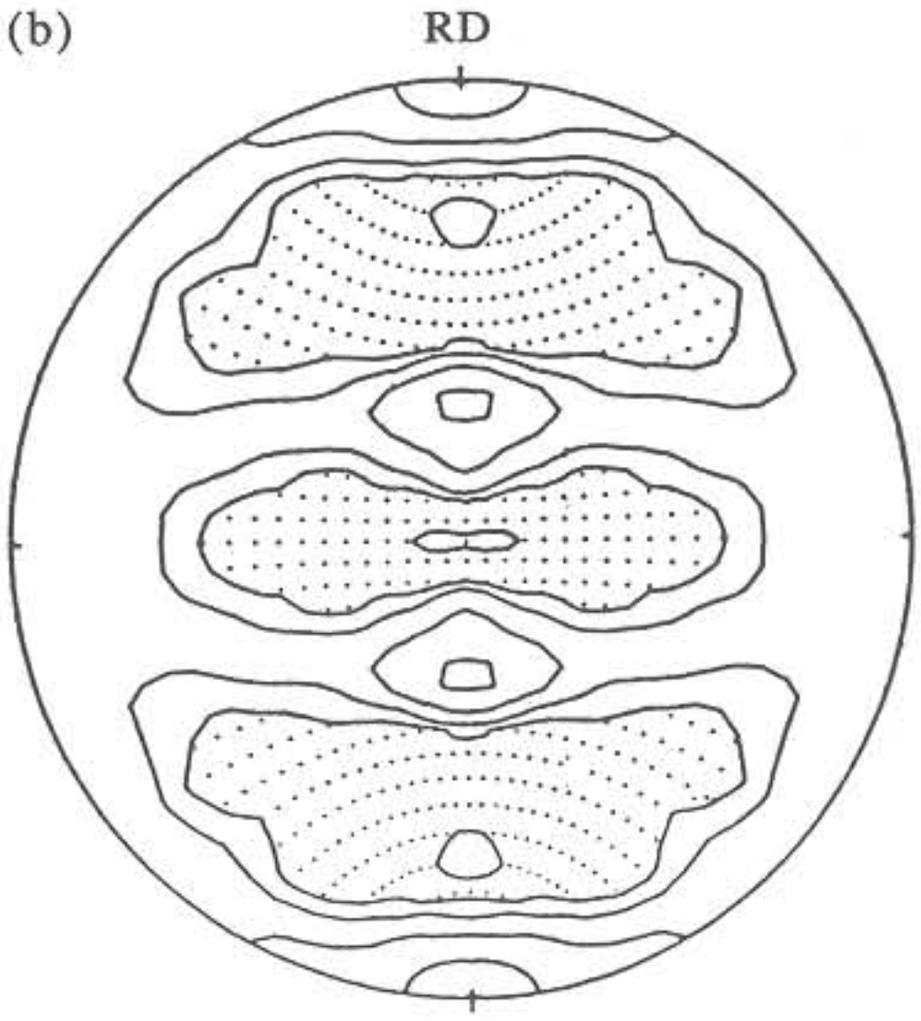

Levels:
0.5 –1 –2 –4 –5.5

Max: 5.6

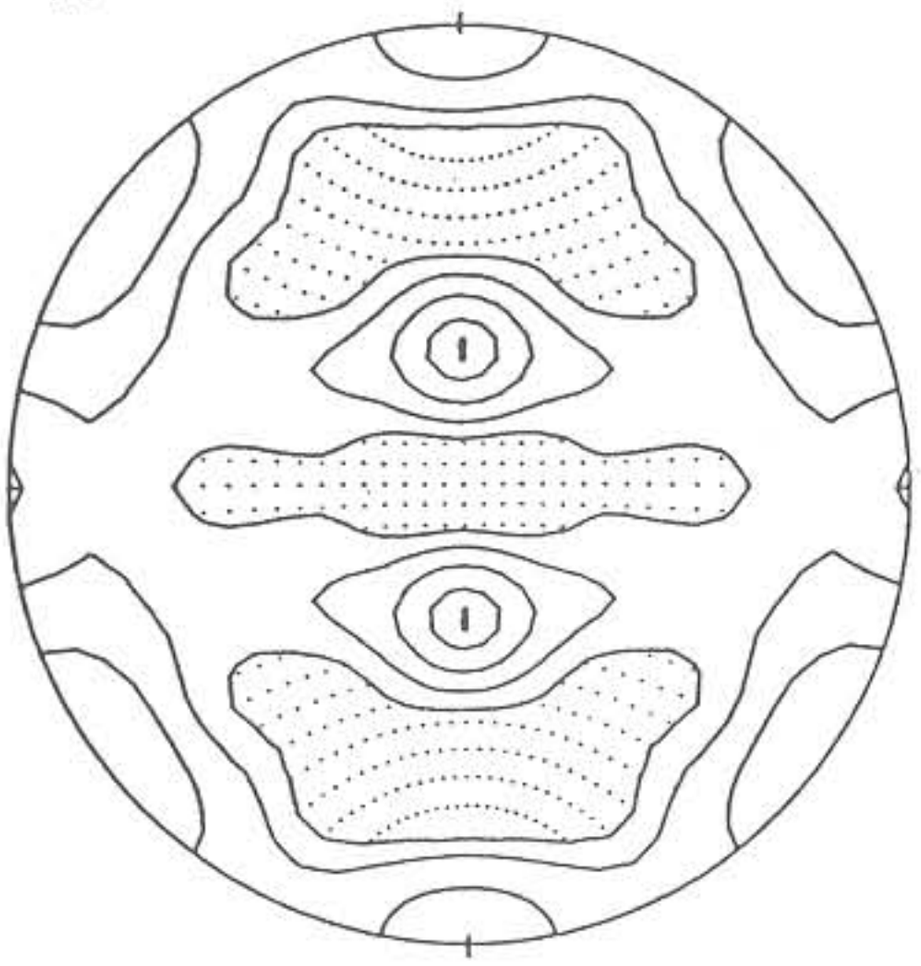

Levels:
0.5 –1 –2 –4 –5.6

Max: 5.7

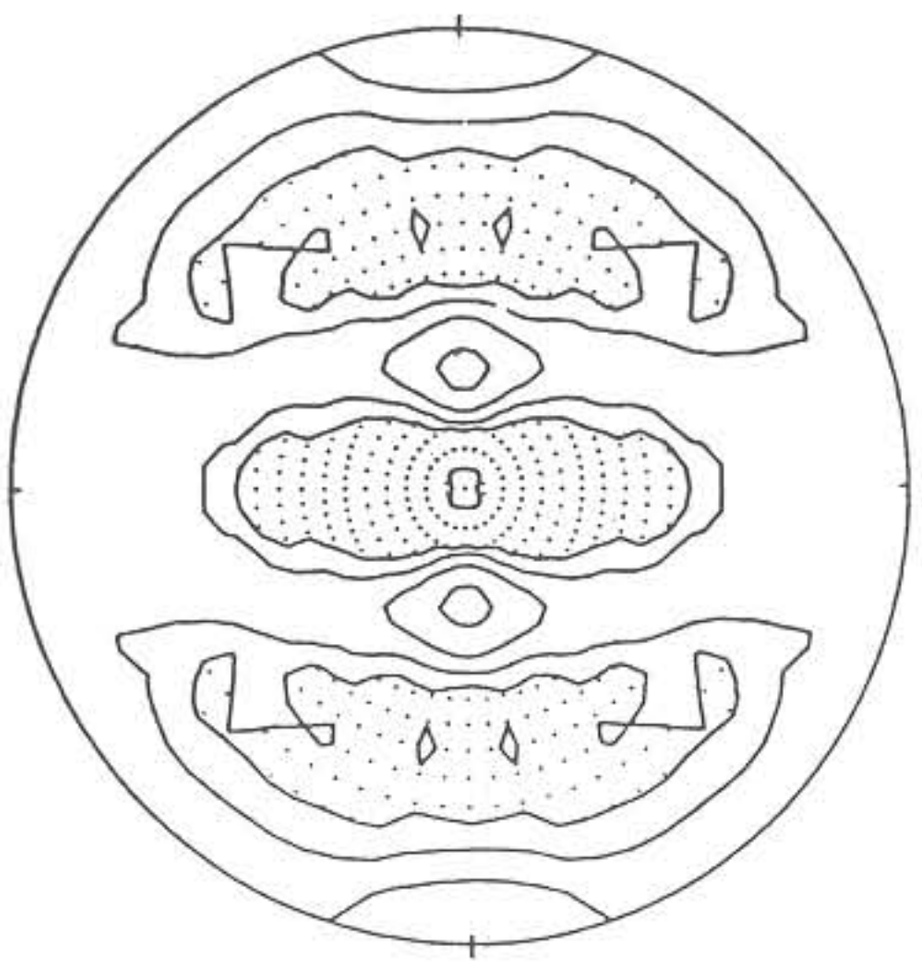

Levels:
0.5 –1 –2 –4

Max: 4.8

Fig. 3. Recalculated {111} pole figures of aluminium and Fe–16% Cr. RD = rolling direction. (a) Aluminium, 75% homogeneously cold rolled, {111} pole figure. (b) Fe–16% Cr, 75% homogeneously cold rolled, data 90° rotated about transverse direction, projection of {111} pole figure. (c) Aluminium, 75% inhomogeneously cold rolled, i.e. sheared, data 90° rotated about transverse direction, {111} pole figure. (d) Fe–16% Cr, 75% inhomogeneously hot rolled, i.e. sheared, projection of {111} pole figure.

which also corresponds to a 90° rotation about T, can now be deduced. Substitution of equation (7) into equations (5a) and (6h) leads to

$$R' \| R + \gamma(R \cdot n_{\text{b.c.c.}}) \cdot b_{\text{b.c.c.}} = R - \gamma(R \cdot b_{\text{f.c.c.}}) \cdot n_{\text{f.c.c.}} \tag{8a}$$

$$N' \| N - \gamma(N \cdot b_{\text{b.c.c.}}) \cdot n_{\text{b.c.c.}} = N + \gamma(N \cdot n_{\text{f.c.c.}}) \cdot b_{\text{f.c.c.}}. \tag{8b}$$

An additional rotation of the orientation 90° about T, which was found experimentally and which transforms R into R^{90} and T into T^{90}, respectively leads to

$$R^{90} = N; \quad R^{90'} = N' \tag{9a}$$

$$N^{90} = -R; \quad N^{90'} = -R' \tag{9b}$$

and thus to

$$R^{90'} = R^{90} + \gamma(R^{90} \cdot n_{\text{f.c.c.}}) \cdot b_{\text{f.c.c.}} \tag{10a}$$

$$N^{90'} = N^{90} - \gamma(N^{90} \cdot b_{\text{f.c.c.}}) \cdot n_{\text{f.c.c.}} \tag{10b}$$

Equations (5a, 6h) and (10a,b) are completely equivalent. That means a rotation of 90° about T transforms the f.c.c. orientation change into that of b.c.c. if the amount of shear γ is the same in the corresponding slip systems. If a f.c.c. orientation (hkl) $[uvw]$ is changed into $(hkl)'$ $[uvw]'$ by slip a b.c.c. orientation $(-u-v-w)$ $[hkl]$ will be changed into $(-u-v-w)'$ $[hkl]'$. Applying the Sachs and the Taylor model it will now be shown that really the equivalent slip systems are activated involving the

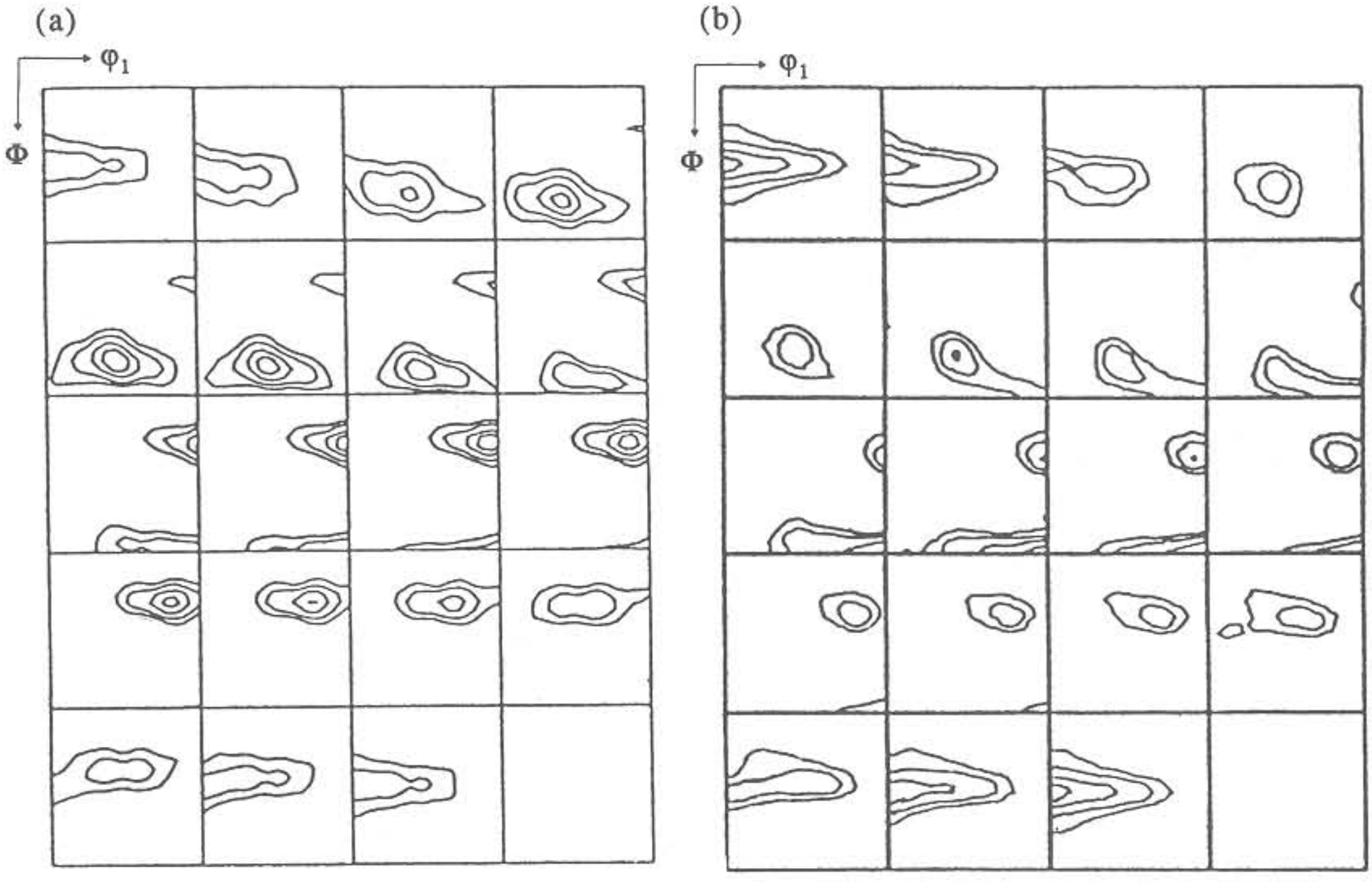

Fig. 4. Orientation distribution functions (ODFs) of aluminium and Fe–16% Cr. (a) Aluminium, 75% homogeneously cold rolled, φ_2-sections. (b) Fe–16% Cr, 75% homogeneously cold rolled, data 90° rotated about transverse direction, φ_2-sections. (c) Aluminium, 75% inhomogeneously cold rolled, i.e. sheared, data 90° rotated about transverse direction, φ_2-sections. (d) Fe–16% Cr, 75% inhomogeneously hot rolled, i.e. sheared, φ_2-sections.

same amount of shear in a f.c.c. as well as in a 90° rotated b.c.c. orientation.

4.2. Equivalence of f.c.c. and b.c.c. deformation in the Sachs model

In the Sachs model of polycrystalline deformation the resolved shear stress τ on a slip system can be calculated from the stress state using the Schmid law. For uniaxial tension stress σ one obtains

$$\tau = m \cdot \sigma, \quad m = \cos(\lambda) \cdot \cos(\kappa) \tag{11}$$

where λ and κ, which define the Schmidfactor m are the angles between the direction of the stress σ and the slip direction and the slip plane normal, respectively. The slip systems with the highest resolved shear stress are activated. The stress state during rolling can be simplified by a tensile stress σ_1 in rolling direction and a compression stress σ_3 of the same magnitude in normal direction ("Tucker" stress state) [11]. The Schmidfactor is then written

$$m = \cos(\lambda_1)\cos(\kappa_1) - \cos(\lambda_3)\cos(\kappa_3) \tag{12a}$$

$$m = (R \cdot n)(R \cdot b) - (N \cdot n)(N \cdot b) \tag{12b}$$

where the subscripts indicate the angles of the stresses in R (1) and in N(3) with respect to the orientation of the slip elements. Changing $n_{\text{f.c.c.}}$ into $b_{\text{b.c.c.}}$ and $b_{\text{f.c.c.}}$ into $-n_{\text{b.c.c.}}$, i.e. transforming f.c.c. glide into b.c.c. glide, and rotating subsequently R into $-N^{90}$ and N into R^{90} according to equations (7, 9) does not change this equation. The $\{110\}\langle 111\rangle$ slip systems in b.c.c. have thus the same resolved shear stress as the 90° about T rotated $\{111\}\langle 110\rangle$ glide systems in f.c.c.

4.3. Equivalence of f.c.c. and b.c.c. deformation in the Taylor model

The strain tensor ϵ^{c} within a crystal due to slip on z slip systems can be calculated for small strains as follows

$$\epsilon^{\text{c}}_{\text{ij}} = \frac{1}{2}\sum_{s=1}^{z} \gamma^{\text{s}}\,(n^{\text{s}}_i b^{\text{s}}_j + n^{\text{s}}_j b^{\text{s}}_i) \tag{13}$$

Rotating the tensor from the crystal system ϵ^{c} into the sample coordinate system ϵ^{a} leads to

$$\epsilon^{\text{a}} = G \cdot \epsilon^{\text{c}} \cdot G^{-1}; \quad G = \begin{pmatrix} u' & v' & w' \\ q' & r' & s' \\ h' & k' & l' \end{pmatrix} \tag{14}$$

where G is the rotation matrix with the normalized components u', v', w' etc. to transform the crystal coordinate system back into the sample coordinate system. If $\epsilon^{\text{a}}_{\text{b.c.c.}}$ is the strain tensor of a b.c.c. orientation, the corresponding strain tensor of a f.c.c. orientation $\epsilon^{\text{a}}_{\text{f.c.c.}}$, additionally rotated 90° about T into $\epsilon^{\text{a,90}}_{\text{f.c.c.}}$ can be calculated as follows

$$\epsilon^{\text{a}}_{\text{f.c.c.}} = -\epsilon^{\text{a}}_{\text{b.c.c.}} \tag{15a}$$

$$\epsilon^{\text{a,90}}_{\text{f.c.c.}} = G_{90} \cdot (-\epsilon^{\text{a}}_{\text{b.c.c.}}) \cdot G_{90}^{-1} \tag{15b}$$

$$\epsilon^{\text{a,90}}_{\text{f.c.c.}} = \begin{pmatrix} 0 & 0 & \bar{1} \\ 0 & 1 & 0 \\ 1 & 0 & 0 \end{pmatrix} \cdot (-\epsilon^{\text{a}}_{\text{b.c.c.}}) \cdot \begin{pmatrix} 0 & 0 & 1 \\ 0 & 1 & 0 \\ \bar{1} & 0 & 0 \end{pmatrix} \tag{15c}$$

G_{90} is the rotation matrix for the 90° rotation about T. This changes the strain tensor $\epsilon^{\text{a}}_{\text{b.c.c.}}$ for the b.c.c. orientation

$$\epsilon^{\text{a}}_{\text{b.c.c.}} = \begin{pmatrix} \epsilon_{11} & \epsilon_{12} & \epsilon_{13} \\ \epsilon_{21} & \epsilon_{22} & \epsilon_{23} \\ \epsilon_{31} & \epsilon_{32} & \epsilon_{33} \end{pmatrix} \tag{16}$$

into $\epsilon^{\text{a,90}}_{\text{f.c.c.}}$ of a 90° rotated f.c.c. orientation

$$\epsilon^{\text{a,90}}_{\text{f.c.c.}} = \begin{pmatrix} -\epsilon_{33} & \epsilon_{32} & \epsilon_{31} \\ \epsilon_{23} & -\epsilon_{22} & -\epsilon_{21} \\ \epsilon_{13} & -\epsilon_{12} & -\epsilon_{11} \end{pmatrix}. \tag{17}$$

During ideal rolling ϵ_{22} is zero (no change of width) and $\epsilon_{33} = -\epsilon_{11}$. That means the strain tensor of a f.c.c. orientation and a 90° rotated b.c.c. orientation differ only in the shear components ϵ_{12} and ϵ_{23}, which are exchanged. Therefore in the Taylor theory the equivalence of the required combination of slip systems in f.c.c. and b.c.c. and thus the occurrence of 90° about T rotated texture components is fulfilled only in case of plane strain deformation.

During rolling of polycrystals however, neither the Sachs nor the ideal Taylor model is completely correct. For low degrees of rolling, i.e. for approximately equiaxed grains the "Full Constraints" Taylor [4] model gives a rather good description of the deformation. With increasing deformation the grains become flat so that the incompatibility in rolling direction is reduced, which leads to a relaxation of the ϵ_{13} tensor component and thus to a decrease of constraints [5]. An orientation which is pronounced by relaxation of this shear in f.c.c. corresponds to a b.c.c. orientation, 90° rotated about T, because it produces the same shear [equations (16, 17)]. But this is not true, if the rolling degree increases. The shear ϵ_{23} is the next one to be relaxed by geometrical reasons. A f.c.c. orientation resulting from this shear corresponds to a 90° T rotated b.c.c. one, which requires a relaxation of ϵ_{12} to be stable and vice versa [equations (16, 17)], which is allowed only in very special cases.

This restriction explains, why rolling textures of polycrystalline f.c.c. and b.c.c. materials cannot be transformed into each other after high deformation by this simple rotation, even if no deformation inhomogeneities are taken into account.

5. EQUIVALENCE OF ROLLING TEXTURES AND SHEAR TEXTURES

A rotation relationship of 90° about T was found also for the stable texture components of the sheared samples with respect to the stable rolling orientations. For rolling at least two sets of slip systems are necessary to keep an orientation stable. In the case of shear, in contrast, only one slip system (or two slip systems which yield the same principal rotation) suffices if it produces the requested strain parallel to the shear plane in shear direction, i.e. here in the case of inhomogeneous rolling parallel to the rolling plane in rolling direction. It is thus obvious, that it will not be possible to connect the path of orientation change like it was done between f.c.c. and b.c.c., although the stable end orientations of rolling and shear can be transformed into each other.

Due to the symmetry of the slip systems every stable and metastable rolling orientation in the Sachs model reveals at least one glide system with a Schmidfactor of zero. The slip plane normal of such a system is perpendicular to N and the slip direction (or the resulting slip direction) is parallel to N. The Schmidfactor m thus changes during rotation about T.

$$m(\omega) = A \cdot \sin(2\omega) + B \cdot \cos(2\omega) \quad A,B = \text{const.} \tag{17}$$

After a rotation of $\omega = 45°$ the slip system with $m = 0$ yields a maximum Schmidfactor and the "Tucker" rolling stress state is changed into a pure shear tensor. Taking also into account the rotation relationship of 45° between rolling and shear coordinates, the 90° rotated slip systems with $m = 0$ in the stable rolling orientations will be those with the highest resolved shear stress in a shear experiment. Because their slip direction is then parallel to the shear direction of the sample (here: rolling direction) no orientation change will occur, i.e. these orientations are stable. Therefore the 90° rotation relationship of the stable orientations of rolling and shear deformation can be explained by the symmetry of the slip systems in the f.c.c. and b.c.c. lattices and not only by the changed stress state.

6. SUMMARY

It was shown that after rolling of f.c.c. and b.c.c. metals strong equivalences in textures appear. Between stable end orientations of both materials a rotation relationship of 90° about the transverse direction (T) exists. This was demonstrated by rotating and adequately presenting the corresponding pole figures and ODFs. Theoretical considerations lead to the same relationship. It is true for rolling of single crystals and polycrystals (Sachs and Taylor model). But for polycrystalline materials some difficulties arise when the constraints of the strain are partly relaxed, especially for the strain ϵ_{23}. The 90° rotation changes ϵ_{23} into ϵ_{12}. The rotation relationship between stable rolling and shear orientations was found experimentally to be 90° too, which was explained by the symmetry of the f.c.c. and b.c.c. slip systems.

REFERENCES

1. G. Wassermann and J. Grewen *Texturen metall. Werkstoffe*, 2nd edn. Springer, Berlin (1962).
2. I. L. Dillamore and W. T. Roberts, *Acta metall.* **12,** 281 (1964).
3. E. Sachs, *Z. Verein Deutsch. Ingen.* **72,** 734 (1928).
4. G. I. Taylor, *J. Inst. Metals* **62,** 307 (1938).
5. H. Honneff and H. Mecking, *Text. of Mater. Proc. ICOTOM* **6,** Iron and Steel Inst. of Japan, Tokyo, p. 347 (1981).
6. H. J. Bunge, *Krista. Technik* **5,** 145 (1970).
7. I. L. Dillamore and H. Katoh, *Metal Sci.* **8,** 21 (1974).
8. H. J. Bunge, *Z. Metallk.* **56,** 872 (1965).
9. B. Sestak and N. Zarubova, *Physica status solidi* **10,** 239 (1965).
10. L. G. Schulz, *J appl. Phys.* **20,** 1030 (1949).
11. G. E. G. Tucker, *J. Inst. Metals* **82,** 655 (1954).